

# Absolute photodetachment cross section measurements of the $O^-$ and $OH^-$ anion

P. Hlavenka, R. Otto, S. Trippel, J. Mikosch, M. Weidemüller, and R. Wester

Citation: *The Journal of Chemical Physics* **130**, 061105 (2009); doi: 10.1063/1.3080809

View online: <https://doi.org/10.1063/1.3080809>

View Table of Contents: <http://aip.scitation.org/toc/jcp/130/6>

Published by the *American Institute of Physics*

---

## Articles you may be interested in

[Photodetachment microscopy of the P, Q, and R branches of the  \$OH^-\$  \( \$v=0\$ \) to  \$OH\(v=0\)\$  detachment threshold](#)  
*The Journal of Chemical Physics* **122**, 014308 (2005); 10.1063/1.1824904

[OH \$^-\$  and OD \$^-\$  threshold photodetachment](#)  
*The Journal of Chemical Physics* **77**, 1153 (1982); 10.1063/1.443980

[High resolution photodetachment study of OH \$^-\$  and OD \$^-\$  in the threshold region 7000–6450 Å](#)  
*The Journal of Chemical Physics* **60**, 1806 (1974); 10.1063/1.1681279

[Cross sections for photodetachment of electrons from negative ions near threshold](#)  
*The Journal of Chemical Physics* **64**, 1368 (1976); 10.1063/1.432404

[Time-of-Flight Mass Spectrometer with Improved Resolution](#)  
*Review of Scientific Instruments* **26**, 1150 (1955); 10.1063/1.1715212

[The cryogenic storage ring CSR](#)  
*Review of Scientific Instruments* **87**, 063115 (2016); 10.1063/1.4953888

---

PHYSICS TODAY

WHITEPAPERS

### ADVANCED LIGHT CURE ADHESIVES

Take a closer look at what these environmentally friendly adhesive systems can do

READ NOW

PRESENTED BY  
 **MASTERBOND**  
ADHESIVES | SEALANTS | COATINGS

# Absolute photodetachment cross section measurements of the O<sup>-</sup> and OH<sup>-</sup> anion

P. Hlavenka, R. Otto, S. Trippel, J. Mikosch,<sup>a)</sup> M. Weidemüller,<sup>b)</sup> and R. Wester<sup>c)</sup>  
*Physikalisches Institut, Universität Freiburg, Hermann-Herder-Straße 3, 79104 Freiburg, Germany*

(Received 7 November 2008; accepted 16 January 2009; published online 13 February 2009)

Absolute total photodetachment cross sections of O<sup>-</sup> and OH<sup>-</sup> anions stored in a multipole radio frequency trap have been measured using a novel laser depletion tomography method. For OH<sup>-</sup> the total cross sections of  $8.5(1)_{\text{stat}}(3)_{\text{syst}}$  and  $8.1(1)_{\text{stat}}(7)_{\text{syst}} \times 10^{-18} \text{ cm}^2$ , measured at 662 and 632 nm, respectively, were found constant in the temperature range of 8–300 K. The O<sup>-</sup> cross sections  $5.9(1)_{\text{stat}}(2)_{\text{syst}}$  and  $6.3(1)_{\text{stat}}(2)_{\text{syst}} \times 10^{-18} \text{ cm}^2$  measured at 170 K at 662 and 532 nm, respectively, agree within error estimations with preceding experiments and increase the accuracy of the widely used calibration standard for relative photodetachment measurements of diverse atomic and molecular species. © 2009 American Institute of Physics. [DOI: 10.1063/1.3080809]

The photodetachment of a weakly bound electron from a neutral molecular core represents a fundamental light-matter interaction. Detached photoelectrons can reveal information on the energy levels in both the anion and the neutral. Comparisons of relative photodetachment cross sections near threshold with Wigner laws allow for precise studies of the long-range electron neutral interaction.<sup>1,2</sup> Time-resolved photoelectron spectroscopy with ultrafast lasers reveals insight into molecular wave packet and electron redistribution dynamics or allows one to probe reactive collisions.<sup>3</sup> Multiphoton detachment in short intense laser pulses provides information on electron-atom interactions in strong laser fields.<sup>4</sup>

Absolute photodetachment cross sections are needed to model the formation and destruction pathways of anions in various plasma environments.<sup>5</sup> The recent detection of negative molecular ions in interstellar clouds<sup>6</sup> emphasizes the need for experimental data to understand the role anions play in interstellar chemistry.<sup>7,8</sup> In such cold and low density environments, anions are expected to be formed by radiative attachment. Photodetachment by stellar and cosmic radiation is likely to be the most efficient destruction channel in photon dominated regions. Since radiative attachment is the inverse process of photodetachment, absolute photodetachment cross section measurements may also help estimate anion formation rates based on the principle of detailed balance.

Photodetachment cross sections have been investigated experimentally and theoretically for a large number of anions. These are—with only few exceptions<sup>9–11</sup>—relative measurements that are brought to an absolute scale by comparing to the cross section of a reference anion. In the majority of experiments this calibration is directly or indirectly traceable to the O<sup>-</sup> anion, thereby relying on only two cross section measurements of Branscomb *et al.*<sup>12</sup> and Lee and Smith.<sup>13</sup> In the former experiment an absolute cross section

was obtained by crossing an ion beam with a broadband light source. The latter measurement was carried out with a selected ion drift tube using normalization to D<sup>-</sup>.

Theoretical predictions of photodetachment cross sections still represent a major challenge. The most recent *ab initio* calculations performed for the atomic anion O<sup>-</sup> by Jian-Hua *et al.*<sup>14</sup> and by Zatsarinny and Bartschat<sup>15</sup> succeeded to reproduce the radiation frequency-dependent shape of the measured O<sup>-</sup> photodetachment cross section. However, a disagreement of ~35% was found when comparing the absolute cross section to experiment. Based on this the authors of Ref. 15 questioned the old measurement of Ref. 12 and suggested to revise the calibration scale. This shows the need for new and independent measurements of the absolute photodetachment cross section of the benchmark anion O<sup>-</sup>.

While O<sup>-</sup> serves as an important benchmark system, the photodetachment of molecular anions yields much more dynamical information. The molecular anion for which the most detailed cross section studies exist is the hydroxyl anion OH<sup>-</sup>. Detailed studies are available for the relative photodetachment cross section of OH<sup>-</sup> in the threshold region using photoelectron spectroscopy. They serve as a precise test of the long-range electron-dipole interaction.<sup>1</sup> Relative cross sections have also been measured for state-specific transitions.<sup>2,16,17</sup> Two absolute cross section measurements have been carried out independently by Branscomb<sup>18</sup> and Lee and Smith.<sup>13</sup> Both measurements were scaled to H<sup>-</sup> and D<sup>-</sup> cross sections and disagree significantly.

In this communication, we report on a series of precise and independent measurements of the absolute photodetachment cross section of the atomic oxygen anion O<sup>-</sup> and the molecular hydroxyl anion OH<sup>-</sup>. Our recently developed technique is based on the interaction of trapped anions with laser light in a temperature-variable multipole radio frequency (rf) ion trap.<sup>11</sup> Importantly, it allows us to obtain absolute photodetachment cross sections of trapped anions without resorting to a calibration procedure. Here we present further im-

<sup>a)</sup>Present address: National Research Council Canada, 100 Sussex Drive, Ottawa, ON K1A 0R6, Canada.

<sup>b)</sup>Present address: Physikalisches Institut, Universität Heidelberg, Philosophenweg 12, 69120 Heidelberg, Germany

<sup>c)</sup>Electronic mail: roland.wester@physik.uni-freiburg.de.

provements that yield a fivefold increase in the experimental accuracy.

The experimental rf ion trap setup has been described in detail in Ref. 19. Its central element is a 22-pole trap<sup>20</sup> that features a large almost field-free volume and is ideally suited for buffer gas cooling of trapped molecular ions to a temperature very near to that of the trap enclosure.<sup>21</sup>

In the photodetachment measurements, anions are depleted by a laser beam propagating parallel to the symmetry axis of the trap with a first-order rate given by Eq. (1) of Ref. 11. The photodetachment depletion rate is proportional to the photodetachment cross section and to the overlap of the ion column density with the photon flux. By scanning the position of the laser beam and measuring the depletion rate at each position the relative ion column density distribution is obtained. Assuming spatial variations of the column density to be small compared to the laser diameter one obtains an explicit formula for the cross section,

$$\sigma_{pd} = \frac{1}{F_L} \int_S k(x,y) ds, \quad (1)$$

where  $F_L$  is the total photon flux and  $k(x,y)$  is the decay rate induced by the laser at the transverse position  $(x,y)$ .<sup>11</sup> In Ref. 11 this integral was derived from a one-dimensional scan of the laser through the trap, relying on cylindrical symmetry for the ion density distribution. In the present setup the integral is obtained from a full two-dimensional tomography of the trapped ions.

Different continuous-wave lasers were employed for the current measurements, a free-running diode laser at 661.9 nm (Mitsubishi ML1J27, 100 mW, spectral width 0.7 nm full width at half maximum), a helium neon laser at 632.8 nm (5 mW), and a single-mode frequency-doubled Nd:YAG (yttrium aluminum garnet) laser at 532 nm (Coherent Verdi, attenuated to 58 mW). Using a thin convex lens ( $f = 1000$  mm) mounted on a step-motor driven two-axis translation stage, the laser beams are imaged to any  $(x,y)$  position in the trap with  $1/e^2$  waists of  $\omega_0 = 350, 210$ , and  $120$   $\mu\text{m}$ , respectively. With a distance from the lens to the trap center of 1104(5) mm, the wavelength-dependent magnification of the image position in the trap with respect to the lens position is calculated. It amounts to 1.109 for 532 nm and 1.097 for 662 nm. A calibrated silicon power meter (Coherent OP2-VIS) is used to determine the laser power in front of the AR-coated vacuum window (99.2% transmission) before and after each measurement. Inside the vacuum chamber the beam propagates without further losses. A photodiode monitors the fluctuation of laser power during the experiment. An electromechanical shutter interrupts the laser beam during the trap injection, cooling, and extraction phases.

Ions are produced in a pulsed supersonic expansion of a suitable precursor gas, crossed by a 1 keV electron beam. For the  $\text{O}^-$  production, normal air is used as precursor gas.  $\text{OH}^-$  stems from rapid chemical conversion of  $\text{NH}_2^-$  by water in a mixture of  $\text{Ar}/\text{NH}_3/\text{H}_2\text{O}$  (88%, 10%, 2%). A bunch of  $\sim 1000$  mass-selected ions is loaded into the trap, which is enclosed by copper housing and temperature-variable between 8 and 300 K. A typical He buffer gas density of

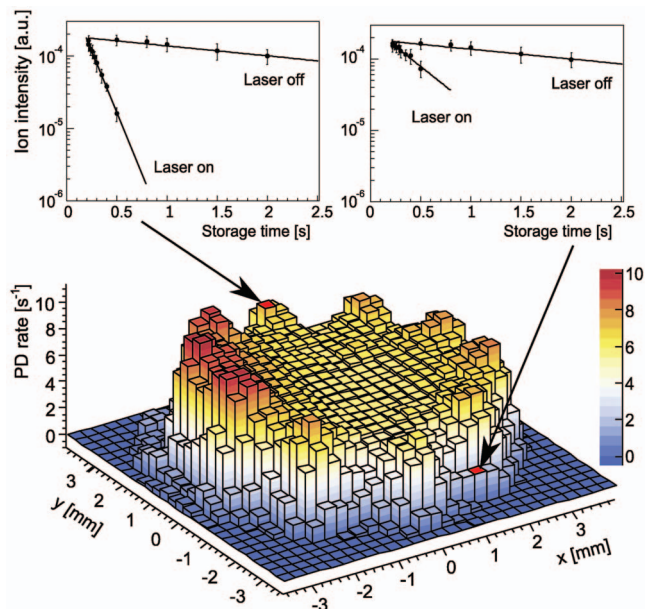


FIG. 1. (Color) Histogram of the measured photodetachment rate for  $\text{O}^-$  as a function of the transverse position of the laser light in the ion trap. The graph reflects the ion density distribution in the 22-pole trap, as the ion column density is proportional to the detachment rate. The insets show two examples for individual loss rate measurements.

$10^{14}$   $\text{cm}^{-3}$  is employed at all temperatures, enhanced by a buffer gas pulse during ion injection. The trap is operated at a frequency of 5 MHz and an amplitude of between 50 V at temperatures below 50 K and 250 V at 300 K. Along the axial direction ions are confined by end electrodes biased to  $-5$  V. To allow good thermalization of the ions, a storage period of 200 ms is inserted before the laser beam is switched on. After a given storage time the signal proportional to the number of ions that survived the interaction with the laser is detected.

To ensure that the laser beam can be moved through the entire ion distribution without clipping at the end electrodes, the ions are, for elevated temperatures, pushed toward the trap center by operation at higher than the usual rf amplitude. To check the full optical access, one-dimensional scans have been carried out at different rf amplitudes in the horizontal and vertical direction. It has been verified that the integral of the measured density distribution is independent of its radial extension. The two-dimensional tomography scans are performed on a mesh with 0.25 mm point spacing. For each laser position the photodetachment rate is obtained in a storage time interval of 0.2–2 s from the difference in the fitted loss rate with and without the laser. The data are averaged over typically four to eight scans thereby traversing the mesh points in random order to avoid systematic drifts.

We have carried out the measurements of the absolute photodetachment cross section of  $\text{O}^-$  and  $\text{OH}^-$  anions at different buffer gas temperatures. Figure 1 shows a typical tomography scan of  $\text{O}^-$  at 300 K. The two insets show the individual detachment rate measurements at two selected mesh points. At 300 K the background ion loss rate of about  $0.25$   $\text{s}^{-1}$  needs to be taken into account; it is mainly caused by the evaporation of ions out of the trap.<sup>22</sup> For lower tem-

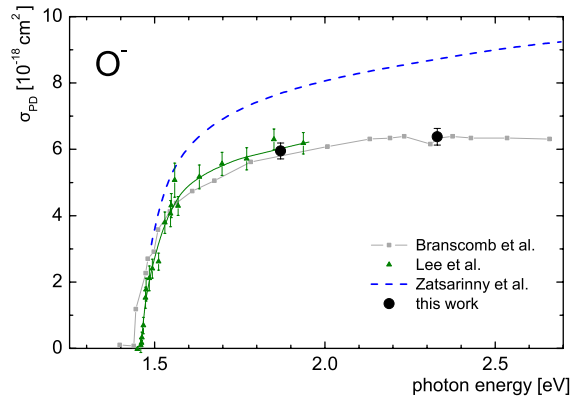


FIG. 2. (Color online) Measured cross section of  $O^-$  as a function of the photon energy. Our data (large full circles) is compared with the relative measurements of Refs. 13 and 25 (squares and small triangles), which were calibrated to hydrogen anion measurements. The dashed line shows the *ab initio* calculation of Ref. 15.

peratures it decreases by orders of magnitude and therefore becomes insignificant.

The photodetachment loss rate for a given position is proportional to the ion column density at that point. Hence, Fig. 1 shows the column density of trapped  $O^-$  in the 22-pole trap. It resolves several interesting features that have not been observed previously. In the center, the ion distribution is relatively uniform. Near the maximum radius of the distribution it increases slightly and shows ten equally spaced maxima as a function of angle. The discussion of these unexpected details of the distribution is the subject of a further publication. We note that for the total cross section measurements the actual shape of the ion distribution is not important (see below).

Following Eq. (1), the absolute photodetachment cross section for  $O^-$  is obtained by discrete integration of the distribution of Fig. 1 and subsequent division by the photon flux. Two measurements at 662 nm, carried out at 300 and 170 K buffer gas temperature, revealed values of  $\sigma = 5.7(2)_{\text{stat}}(2)_{\text{syst}}$  and  $5.9(1)_{\text{stat}}(2)_{\text{syst}} \times 10^{-18} \text{ cm}^2$ . The estimation of the statistical and systematic accuracies, which is discussed below, shows that these two values agree with each other. At 532 nm we obtain  $\sigma = 6.3(1)_{\text{stat}}(2)_{\text{syst}} \times 10^{-18} \text{ cm}^2$ , measured at 170 K (depicted in Fig. 2). These results pertain to  $O^-$  in a mixture of the two  $^2P_{3/2}$  and  $^2P_{1/2}$  spin-orbit states, which are spaced by  $177.13 \text{ cm}^{-1}$ .<sup>23</sup>

For  $OH^-$  we have measured the absolute cross section for laser wavelengths of 662 and 632.8 nm and for different temperatures from 8 to 300 K (see Fig. 3). The measurement with the 20 times weaker HeNe laser relies on the normalized column density distribution known from the 662 nm tomography. In this case the cross section is calculated from the measured decay rate at the trap center  $k_{\text{HeNe}}(x=0, y=0)$  and known density  $\rho(0,0) = k_{662}(0,0) / \int k_{662}(x,y)$ , and is hence subject to a larger error. As seen in Fig. 3, our measurements reveal no change of the  $OH^-$  photodetachment cross section in the range of 8–300 K at these wavelengths. The temperature-averaged cross sections are  $\sigma_{pd}(662 \text{ nm}) = 8.5(1)_{\text{stat}}(3)_{\text{syst}} \times 10^{-18} \text{ cm}^2$  and  $\sigma_{pd}(632 \text{ nm}) = 8.1(1)_{\text{stat}}(7)_{\text{syst}} \times 10^{-18} \text{ cm}^2$ .

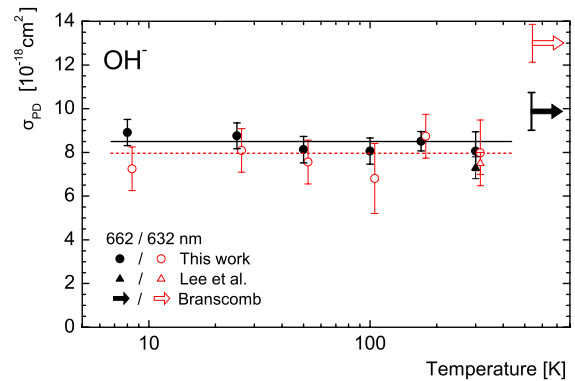


FIG. 3. (Color online) Measured photodetachment cross sections of  $OH^-$  at 662 nm (solid symbols) and 632.8 nm (open symbols) at different temperatures. The data points for 632.8 nm are slightly shifted horizontally for clarity. The horizontal lines represent the temperature-averaged values. The values of Ref. 13 are marked by the triangles and the values of Ref. 18, obtained at unknown internal temperature, are indicated by the arrows.

To assess the accuracy of the measured cross sections we consider both statistical and possible systematic errors. The statistical fluctuations of the measured ion intensities amount to about 7%, limited by noise in the microchannel plate detector and shot noise due to the finite number of ions. This leads to an uncertainty of the fitted decay rates of  $<2\%$  for the majority of the exponential fits. The statistical uncertainty of the integral in Eq. (1) is hence estimated to be 1.5%, which is further improved by averaging over several tomography scans. A systematic source of error of the integral is the accuracy of the beam positioning. The translation stage, which carries the imaging lens, can be positioned with micrometer precision. The accuracy of the magnification is determined by the uncertainty of the lens-to-trap distance and the uncertainty of the focal length of the lens. For this we measure a value of below 1%. The overall accuracy of the position is therefore estimated to be 1% for each dimension. The absolute laser power is determined with a power meter before the beam enters vacuum chamber. Taking into consideration the nominal accuracy of the silicon-based power meter and possible clipping of the laser beam on the detector surface the accuracy of the laser power measurement is better than 2%. The vacuum viewport through which the beam is passed into the trap setup is antireflection coated with an absorption below the power meter resolution. Possible power changes due to clipping at the entrance electrode of the trap or backscattering at the exit electrode are estimated to lie below 0.3%. Relative fluctuations during a tomography scan are continuously monitored with a power meter behind one port of a beam splitter. To judge the systematic error of the finite discretization of the tomography mesh we performed numerical simulations. They show that for the experimental conditions this error is below 0.3%. Measurements with different ion density distributions, created by using different rf amplitudes, verify that the cross section derivation is not sensitive to the details of the distribution. Accordingly, the overall accuracy for determining the absorption cross section from a tomography scan is given by 1.5% statistical error and 3.5% systematic error, containing 2% for the laser power



and 1.5% for the two position coordinates. A larger uncertainty is derived for the OH<sup>-</sup> measurements with the HeNe laser, which is cross-referenced to the 662 nm measurement.

The majority of previous photodetachment cross section measurements have been scaled using the O<sup>-</sup> anion as reference, relying on the only two cross section measurements of Branscomb and Smith<sup>9</sup> and Lee and Smith,<sup>13</sup> both independently scaled to the H<sup>-</sup> (D<sup>-</sup>) cross section. In Fig. 2 we compare their data with our absolute measurements. Our values are in excellent agreement with these previous, many decades-old experiments. However, the recent *ab initio* calculation gives values that are about 35% too high.<sup>15</sup> Considering the high accuracy of our new measurements this deviation clearly asks for an explanation.

The measured photodetachment cross section of the OH<sup>-</sup> anion  $\sigma = 8.5(1)_{\text{stat}}(3)_{\text{syst}} \times 10^{-18} \text{ cm}^2$  at 662 nm agrees within two sigma with both previous values of  $9.8(9) \times 10^{-18} \text{ cm}^2$  (Ref. 18) and  $7.3(5) \times 10^{-18} \text{ cm}^2$ ,<sup>13</sup> and thereby somewhat reconciles the latter two values. With our previous value,<sup>11</sup> which had a much larger uncertainty due to the employed one-dimensional tomography, we also find fair agreement. The data for different temperatures prove that within the error bar the cross section stays constant in the temperature range from 8 to 300 K (see Fig. 3). Since the thermal population of rotational states in OH<sup>-</sup> changes strongly in this range, this is evidence for a rotational state-independent cross section for *J* between zero and about five, in agreement with the Hönl-London factors for *s*-wave detachment.<sup>24</sup>

In this communication we report measurements of absolute photodetachment cross sections at several laser wavelengths for O<sup>-</sup> and OH<sup>-</sup> stored in a multipole rf trap at several different temperatures. Absolute cross section measurements with 1.5% statistical and 3.5% systematic accuracy are achieved. Our measurements validate the reliability of the previous O<sup>-</sup> cross section used as a normalization standard<sup>12,13</sup> and improve the accuracy of future calibrations to O<sup>-</sup>. The measured OH<sup>-</sup> photodetachment cross section shows no temperature dependence and therefore no rotational state dependence. In the future we plan to use this method to study the photodetachment of larger anions and to

provide accurate cross sections for use in models of the molecular abundance in the interstellar medium.

This work was supported by the Deutsche Forschungsgemeinschaft under Contract No. WE 2592/2-1. P.H. acknowledges support by the Alexander von Humboldt foundation.

- <sup>1</sup>P. A. Schulz, R. Mead, P. Jones, and W. Lineberger, *J. Chem. Phys.* **77**, 1153 (1982).
- <sup>2</sup>J. R. Smith, J. B. Kim, and W. C. Lineberger, *Phys. Rev. A* **55**, 2036 (1997).
- <sup>3</sup>A. Stolow, A. E. Bragg, and D. M. Neumark, *Chem. Rev. (Washington, D.C.)* **104**, 1719 (2004).
- <sup>4</sup>R. Reichle, H. Helm, and I. Y. Kuyan, *Phys. Rev. Lett.* **87**, 243001 (2001).
- <sup>5</sup>S. Petrie and D. K. Bohme, *Mass Spectrom. Rev.* **26**, 258 (2007).
- <sup>6</sup>M. C. McCarthy, C. A. Gottlieb, H. Gupta, and P. Thaddeus, *Astrophys. J.* **652**, L141 (2006).
- <sup>7</sup>E. Herbst, *Nature (London)* **289**, 656 (1981).
- <sup>8</sup>S. Petrie and E. Herbst, *Astrophys. J.* **491**, 210 (1997).
- <sup>9</sup>L. M. Branscomb and S. J. Smith, *Phys. Rev.* **98**, 1028 (1955).
- <sup>10</sup>P. Balling, C. Brink, T. Andersen, and H. K. Haugen, *J. Phys. B* **25**, L565 (1992).
- <sup>11</sup>S. Trippel, J. Mikosch, R. Berhane, R. Otto, M. Weidemüller, and R. Wester, *Phys. Rev. Lett.* **97**, 193003 (2006).
- <sup>12</sup>L. M. Branscomb, D. S. Burch, S. J. Smith, and S. Geltman, *Phys. Rev.* **111**, 504 (1958).
- <sup>13</sup>L. C. Lee and G. P. Smith, *J. Chem. Phys.* **70**, 1727 (1979).
- <sup>14</sup>W. Jian-Hua, Y. Jian-Min, and V. K. Lan, *Chin. Phys.* **12**, 1390 (2003).
- <sup>15</sup>O. Zatsarinny and K. Bartschat, *Phys. Rev. A* **73**, 022714 (2006).
- <sup>16</sup>C. Delsart, F. Goldfarb, and C. Blondel, *Phys. Rev. Lett.* **89**, 183002 (2002).
- <sup>17</sup>F. Goldfarb, C. Drag, W. Chaibi, S. Kröger, C. Blondel, and C. Delsart, *J. Chem. Phys.* **122**, 014308 (2005).
- <sup>18</sup>L. M. Branscomb, *Phys. Rev.* **148**, 11 (1966).
- <sup>19</sup>J. Mikosch, U. Fröhling, S. Trippel, R. Otto, P. Hlavenka, D. Schwalm, M. Weidemüller, and R. Wester, *Phys. Rev. A* **78**, 023402 (2008).
- <sup>20</sup>D. Gerlich, *Phys. Scr.* **T59**, 256 (1995).
- <sup>21</sup>J. Glosík, P. Hlavenka, R. Plašil, F. Windisch, D. Gerlich, A. Wolf, and H. Kreckel, *Philos. Trans. R. Soc. London, Ser. A* **364**, 2931 (2006).
- <sup>22</sup>J. Mikosch, U. Fröhling, S. Trippel, D. Schwalm, M. Weidemüller, and R. Wester, *Phys. Rev. Lett.* **98**, 223001 (2007).
- <sup>23</sup>D. M. Neumark, K. R. Lykke, T. Andersen, and W. C. Lineberger, *Phys. Rev. A* **32**, 1890 (1985).
- <sup>24</sup>P. A. Schulz, R. D. Mead, and W. C. Lineberger, *Phys. Rev. A* **27**, 2229 (1983).
- <sup>25</sup>L. M. Branscomb, S. J. Smith, and G. Tisone, *J. Chem. Phys.* **43**, 2906 (1965).